AIMS Mathematics, 9(1): 1323–1345.
DOI: 10.3934/math.2024065
Received: 03 October 2023
Revised: 09 November 2023
Accepted: 12 November 2023
Published: 07 December 2023

http://www.aimspress.com/journal/Math

Research article

Traveling-wave and numerical solutions to nonlinear evolution equations via modern computational techniques

Abdulghani R. Alharbi*

Department of Mathematics, College of Science, Taibah University, Al-Madinah Al-Munawarah 42353, Saudi Arabia

* **Correspondence:** Email: arharbi@taibahu.edu.sa, abdul928@hotmail.com.

Abstract: In this research, we apply some new mathematical methods to the study of solving couple-breaking soliton equations in two dimensions. Soliton solutions for equations with free parameters like the wave number, phase component, nonlinear coefficient and dispersion coefficient can be obtained analytically by adding trigonometric, rational and hyperbolic functions. We will also look into how two-dimensional diagrams are affected by the wave phenomena, illustrating the answers with a mix of two- and three-dimensional graphs. The proposed system will be transformed into a numerical system by using the finite difference method to simulate Black-Scholes equations numerically. Furthermore, we will evaluate the stability and accuracy of the numerical findings by making analytical and graphical comparisons with precise solutions and we will talk about the error analysis of the numerical scheme. All forms of nonlinear evolutionary systems can benefit from the methods utilized in this work because they are sufficient and acceptable.

Keywords: couple-breaking soliton equations; solitary solutions; numerical solutions; finite differences; stability; accuracy
Mathematics Subject Classification: 35A24, 35B35, 35Q51, 35Q92, 65N06, 65N40, 65N45, 65N50

1. Introduction

The pursuit of numerical and soliton solutions for nonlinear partial differential equations is a challenging topic in mathematical physics. Nonlinear partial differential equations are used extensively in the field of analysis to study nonlinear systems. These equations are valuable in various scientific domains. There are a lot of numerical and analytical methods that are used to find solutions, including the exp-function and (P/Q)-expansion [1–13]. Several methodologies have been used to investigate the equations presented to obtain soliton solutions for nonlinear partial differential equations.

In their study, Zaki [14] provided single-wave solutions with positive and negative amplitudes

that have the same widths, positive speeds and positive phase shifts. Wazwaz [15] investigated the Kadomtsev-Petviashivilli-modified equal width equatio by using the tanh and sine-cosine methods, revealing distinct exact solutions, including solitary wave and periodic solutions. This approach has been previously documented in various works [15–17]. In 1995, Radha and Lakshmanan examined the localized structures inside of a pair of couple-breaking soliton equations, as well as investigated the presence of the Painleve property [18]. In recent years, Radha and Lakshmanan [18] conducted a study on the existence of exponentially localized systems in a (2 + 1)-dimensional pair Bogoliubov-de Gennes equation and its relationship to the Painleve property. Yan and Zhang [19] have developed families of solutions for the two-and-a-half-dimensional plus one-dimensional Benjamin-Ono-Schmidt problem and they exhibit soliton-like behavior. Chen et al. (2003) employed the newly acquired generalized expansion strategy of the Riccati problem to obtain a soliton solution for the (2 + 1)-dimensional pair couple-breaking soliton equation after the elapse of a one-year period [20].

In their study, Wang et al. [21] were able to derive the three-component coupled Hirota hierarchy by utilizing the dressing approach. In their paper, Tian et al. [22] introduced a method that effectively and directly addresses the symmetry-preserving discretization of a specific group of generalized higher-order equations. Additionally, they presented an unresolved issue pertaining to the relationship between symmetries and the multipliers of conservation law. Furthermore, Li et al. [23] successfully addressed the Cauchy problem associated with the generic n-component nonlinear Schrödinger equations, providing the N-soliton solutions. Additionally, a hypothesis regarding the phenomenon of nonlinear wave propagation was put up. Nonlinear partial differential equations are solved by using various techniques, which are generally associated with the wave function ansatz approach. However, it is essential to note that these strategies have certain limitations and restrictions. The interested reader may consult the references provided by Dong [24, 25]. The nonlinear partial differential equation has garnered significant attention in recent academic research [26–32]. In their study, Peng and Krishnan [33] employed the singular manifold approach to investigate two novel types of accurate soliton solutions for the two-and-a-half-dimensional pair Bose-Einstein condensate scattering problem. In a study conducted by Inan (2010), the researcher investigated the two-and-a-half-dimensional pair couple breaking soliton equation by using the approach of generalized Jacobi elliptic functions [34]. The problem under consideration yielded periodic and numerous soliton solutions as a consequence of the inquiry conducted. Furthermore, Cheng and Chen [35] successfully derived the nonlocal symmetry obtained from the Lax pair, in addition to the residual symmetry associated with the truncated Painleve expansion. Osman [36] successfully derived the multiple-soliton solutions to the two-dimensional-pair couple-breaking soliton problem by using the generalized unified technique. The answers were derived in order to address the challenge at hand. In recent years, a considerable number of scholars have conducted extensive research on diverse analytical approaches pertaining to the (2 + 1)-dimensional pair couple breaking soliton model. The scholars in question originate from many academic disciplines. Various techniques have been employed to address the problem of the two-dimensional-pair couple-breaking soliton. These methodologies include the Hirota bilinear methodology [37], the similarity modification process [38] and the cos-Gordon expansion method [39], among others. Numerous methodologies have been amalgamated to provide a singular and definitive solution. In recent research, Alharbi [40] employed the parabolic Monge-Ampere technique to provide the numerical solution for the two-dimensional fourth-order parabolic thin-film equation. In their study, Ren and Chu (2021) examined soliton molecules and investigated the generalized Bogoliubov-de Gennes equations in both

two-dimensional and one-dimensional systems [41]. The research was conducted by the authors. To the best of our knowledge, existing literature does not contain any documented solution to the (2 + 1)-dimensional Zakharov-Kuznetsov modified equa-width equations and a few couple-breaking soliton equations by using the method proposed in this study. Furthermore, the data presented in this paper might serve as a supplementary resource for other publications pertaining to the same overarching subject matter. Furthermore, we have initiated the development of a solution that integrates hyperbolic and trigonometric function solutions, incorporating free parameters. The solutions to these difficulties will have broad applications in scientific research, maritime engineering and other disciplines. The Kudryashov technique utilizes the transformed rational function approach proposed by Kaplan and Akbulut [42] and leverages the coefficient of variation to analyze the behavior of generalized breaking solitons, as discussed by Qin [43]. Kumar [44] conducted a study on the generalized Schrodinger equation, while Mirzazadeh et al. [45] examined the Jaulent-Miodek equation. Additionally, Xia and Xiong [46] researched fractional partial differential equations. In their study, Alharbi et al. [47] effectively addressed the Kadomtsev-Petviashvili problem by employing the adaptive moving mesh technique. Alharbi [48] focused on examining the structures of traveling waves and exploring their stability and accuracy in the context of two-dimensional Riemann problems. Ma [49] focused on the soliton solutions of the nonlocally integrable modified Korteweg-de Vries problem. Additionally, he explored the inverse scattering transformations and soliton solutions of nonlocal integrable equations by employing the Riemann-Hilbert problems derived from the one-group reduction technique [50].

The couple-breaking soliton system, as discussed by various scholars [35, 36], is often regarded as follows:

$$\begin{aligned} &\Gamma_t + 4\beta\Gamma\Psi_x + 4\beta\Gamma_x\Psi + \beta\Gamma_{xxy} = 0, \\ &\Psi_x - \Gamma_y = 0. \end{aligned} \tag{1.1}$$

Bogoyovlenskii [51] is credited with the initial introduction of this equation. In 1996, Calogero and Degasperis [52, 53] utilized the (2 + 1)-dimensional coupled couple-breaking soliton equation to describe the interaction between a Riemann wave propagating down the y axis and a long wave propagating along the x axis. The application of the equation to the matter of the Riemann wave was employed to achieve this. The wave phenomena represented by the equations play a crucial role in preserving the coherence of water wave occurrences and ensuring close interaction. This discovery has the potential to facilitate additional investigations into nonlinear wave phenomena, which hold considerable importance within the domain of ocean engineering. In their study, Kazeykina and Klein [54] conducted an examination wherein they examined the stability of solutions for a specific equation and presented numerical solutions for said problem. The Kansa technique [55] was employed to assess the quantitative implications of the proposed system. However, a comprehensive examination of the system's stability and an error analysis of the numerical method employed in system (1.1) have yet to be undertaken. Engaging in more research is necessary in order to enhance our understanding of this particular topic matter. The fundamental objective of this research is to obtain several analytic solutions to a problem represented by Eq (1.1) through the utilization of modified S-expansion and generalized algebraic techniques. To achieve the desired objective, the numerical solution has been integrated with finite differences to generate numerical outcomes for the investigated system. We have significantly contributed to the understanding of physical issues in practical applications through a comprehensive analysis and visual comparison of solutions to traveling-wave problems, as well as the corresponding numerical results.

The subsequent sections of this essay will be presented in outline format. Section 2 provides a comprehensive analysis of mathematical models, offering a broad perspective on the subject matter. The third section of this paper presents the methodology that has been established to extract results from nonlinear partial differential squations. The numerical methods employed to compute the numerical solutions of the proposed system (1.1) are outlined in Section 4. This section also provides comprehensive information on the stability, accuracy and convergence properties of these numerical methods. Subsequently, we proceeded to manipulate the given equations in order to obtain a diverse range of solutions for the differential equation collection. The subsequent section of this paper will go into the graphical and physical elucidations of the selected solutions. A juxtaposition of the responses is exhibited in the subsequent section (Section 5) and the final remarks are expounded upon in the subsequent section (Section 6).

2. Overview of proposed procedures

The expression below represents the development equation for $\Gamma(x, y, t)$ and $\Psi(x, y, t)$, which depend on x, y and t.

$$G_1(\Gamma_t, \Gamma_x, \Gamma_y, \Gamma_{xxy}, \Psi, \Psi_y, \Psi_x \dots) = 0. \tag{2.1}$$

Step 1. The traveling-wave solutions of system (1.1) are obtained via the following procedure:

$$\begin{aligned} \Gamma(x, y, t) &= \Phi(\zeta), \qquad \zeta = x + y - \alpha t, \\ \Psi(x, y, t) &= \Theta(\zeta), \end{aligned} \tag{2.2}$$

where α represents the speed of the wave.

Step 2. The subsequent ordinary differential equation (ODE) reflects the nonlinear evolution equation denoted as Eq (2.1):

$$G_2(\Phi, \Phi_\zeta, \Phi_{\zeta\zeta\zeta}, \Theta, \Theta_\zeta, \dots) = 0, \tag{2.3}$$

where G_2 is a polynomial in terms of $\Theta(\zeta)$, $\Phi(\zeta)$ and their respective derivatives.

The generalized indirect algebraic technique proposes that the solution to Eq (2.3) is as follows:

$$\Phi(\zeta) = p_0 + \sum_{k=1}^{M} \left(p_k \psi(\zeta)^k + \frac{s_k}{\psi(\zeta)^k} \right), \tag{2.4}$$

where $\psi(\zeta)$ represents a solution of the following equation:

$$\psi'(\zeta) = \left(\sum_{k=0}^{4} \gamma_k \psi^k(\zeta) \right)^{\frac{1}{2}}. \tag{2.5}$$

The values of p_k and s_k are yet to be determined, while M is a positive integer that serves to balance the greatest degree of the nonlinear terms and the highest order of the derivatives. The values of γ_k, where $0 \le k \le 4$, are presented in Table 1 as reported in the reference [56].

Table 1. Associations between the variable γ_k, where $0 \le k \le 4$ and the function $\psi(\zeta)$.

$(\gamma_0, \gamma_1, \gamma_2, \gamma_3, \gamma_4)$	$\psi(\zeta)$
$\left(\gamma_0 = \frac{\gamma_2^2}{4\gamma_4}, \gamma_1 = 0, \gamma_2 < 0, \gamma_3 = 0, \gamma_4 > 0\right)$	$\psi(\zeta) = \sqrt{-\frac{\gamma_2}{2\gamma_4}} \tanh\left(\sqrt{-\frac{\gamma_2}{2}}\zeta\right).$
$(\gamma_0 = 0, \gamma_1 = 0, \gamma_2 > 0, \gamma_3 = 0, \gamma_4 < 0)$	$\psi(\zeta) = \sqrt{-\frac{\gamma_2}{\gamma_4}} \operatorname{sech}\left(\sqrt{\gamma_2}\zeta\right).$
$\left(\gamma_0 = \frac{\gamma_2^2}{4\gamma_4}, \gamma_1 = 0, \gamma_2 > 0, \gamma_3 = 0, \gamma_4 > 0\right)$	$\psi(\zeta) = \sqrt{\frac{\gamma_2}{2\gamma_4}} \tan\left(\sqrt{\frac{\gamma_2}{2}}\zeta\right).$
$(\gamma_0 = 0, \gamma_1 = 0, \gamma_2 = 0, \gamma_3 = 0, \gamma_4 > 0,)$	$\psi(\zeta) = -\frac{1}{\sqrt{\gamma_4}\zeta}.$
$(\gamma_0 = 0, \gamma_1 = 0, \gamma_2 < 0, \gamma_3 = 0, \gamma_4 > 0)$	$\psi(\zeta) = \sqrt{-\frac{\gamma_2}{\gamma_4}} \sec\left(\sqrt{-\gamma_2}\zeta\right).$
$(\gamma_0 = 0, \gamma_1 = 0, \gamma_2 > 0, \gamma_3 \neq 0, \gamma_4 = 0)$	$\psi(\zeta) = -\frac{\gamma_2}{\gamma_3} \operatorname{sech}^2\left(\frac{\sqrt{\gamma_2}}{2}\zeta\right).$

The modified S-expansion method provides the following solution to Eq (2.3):

$$\psi(\zeta) = \lambda_0 + \sum_{k=1}^{N} \left(\lambda_k S(\zeta)^k + \frac{q_k}{S(\zeta)^k}\right), \tag{2.6}$$

where $S(\zeta)$ represents a solution of the following equation:

$$S'(\zeta) = \mu_0 + \mu_1 S(\zeta) + \mu_2 S(\zeta)^2, \tag{2.7}$$

where the values of μ_k, where $0 \le k \le 2$, can be found in Table 2 [57]. The values of q_k and λ_k will be determined at a later stage.

Table 2. Relationships between μ_k, $0 \le k \le 2$ and the function $S(\zeta)$.

(μ_0, μ_1, μ_2)	$S(\zeta)$
$(\mu_0 = 0.5, \mu_1 = 0.0, \mu_2 = 0.5)$	$S(\zeta) = \sec(\zeta) + \tan(\zeta), \csc(\zeta) - \cot(\zeta).$
$(\mu_0 = 0.5, \mu_1 = 0.0, \mu_2 = 0.5)$	$S(\zeta) = \sec(\zeta) - \tan(\zeta), \csc(\zeta) + \cot(\zeta).$
$(\mu_0 = \pm 1, \mu_1 = 0.0, \mu_2 = \pm 1)$	$S(\zeta) = \tan(\zeta), \cot(\zeta).$
$(\mu_0 = 0.0, \mu_1 = 1.0, \mu_2 = -1.0)$	$S(\zeta) = \frac{1}{2}\left(1 + \tanh\left(\frac{1}{2}\zeta\right)\right).$
$(\mu_0 = 1.0, \mu_1 = 0.0, \mu_2 = -1.0)$	$S(\zeta) = \tanh(\zeta), \coth(\zeta).$
$(\mu_0 = 1/2, \mu_1 = 0.0, \mu_2 = -1/2)$	$S(\zeta) = \tanh(\zeta) \pm \operatorname{sech}(\zeta), \coth(\zeta) \pm \operatorname{csch}(\zeta).$

3. Methodology

Consider the couple-breaking soliton equations in the (2 + 1)-dimensional space

$$\begin{aligned} &\Gamma_t + 4\beta\Gamma\Psi_x + 4\beta\Gamma_x\Psi + \beta\Gamma_{xxy} = 0, \\ &\Psi_x - \Gamma_y = 0 \end{aligned} \tag{3.1}$$

as a partial differential equations system with unknown functions $\Gamma = \Gamma(x, y, t)$ and $\Psi = \Psi(x, y, t)$. When the transformations are applied, Eq (3.1) is reduced to an ODE system.

$$\begin{aligned} \Gamma(x,y,t) =& \Phi(\zeta), \qquad \zeta = x + y - \alpha\, t, \\ \Psi(x,y,t) =& \Theta(\zeta). \end{aligned} \tag{3.2}$$

Consequently, the equations making up Eq (3.1) are given by

$$\begin{aligned} -\alpha\, \Phi_{\zeta} + 4\beta \Phi\, \Theta_{\zeta} + 4\beta \Phi_{\zeta}\, \Theta + \beta\, \Phi_{\zeta\zeta\zeta} = 0, \\ \Theta_{\zeta} - \Phi_{\zeta} = 0. \end{aligned} \tag{3.3}$$

By performing the integration of the second equation in Eq (3.3) with respect to the variable ζ, we obtain the following result: $\Theta = \Phi$. Hence, the first equation in Eq (3.3) can be expressed as

$$-\alpha\, \Phi + 4\beta\, \Phi^2 + \beta\, \Phi_{\zeta\zeta} = 0. \tag{3.4}$$

The value of $M = 2$ in Eq (3.4) is established by achieving equilibrium between $\Phi_{\zeta\zeta}$ and Φ^2.

The solution to Eq (3.4) can be obtained by using the modified S-expansion method with $M = 2$ as follows

$$\psi(\zeta) = \lambda_0 + \lambda_1 S(\zeta) + \frac{q_1}{S(\zeta)} + \lambda_2 S(\zeta)^2 + \frac{q_2}{S(\zeta)^2}, \tag{3.5}$$

where $S(\zeta)$ represents a solution of the following equation:

$$F'(\zeta) = \mu_0 + \mu_1 S(\zeta) + \mu_2 S(\zeta)^2. \tag{3.6}$$

The values of μ_i for $i = 0, 1, 2$ are presented in Table 2. To investigate the analytical solutions to the differential equation given by Eq (3.4), it is necessary to adhere to the following procedure.

(1) A set of equations may be derived for the variables $\lambda_0,\ \lambda_m,\ q_m$, where $m = 1, 2$, by combining Eqs (3.5) and (3.6) with Eq (3.4) and equating the coefficients of $S(\zeta)^m$, where $-4 \le m \le 4$, to zero.
(2) Utilize mathematical tools, such as Mathematica or Maple, to solve the resultant system.
(3) By inserting the values of $\mu_0,\ \mu_1$ and μ_2 into Eq (3.5) together with the function $S(\zeta)$ from Table 2 and further substituting $\lambda_0,\ \lambda_k,\ q_k, k = 1, 2$, several trigonometric functions and rational solutions to Eq (3.4) may be derived.

After completing the previous steps, we determine the values of λ_0, λ_1, λ_2, q_1, q_2 and α.

(1) Assume that $\mu_0 = 0, \mu_1 = \pm 1$ and $\mu_2 = \mp 1$; hence, the solutions of Eq (1.1) Γ, as follows

$$\begin{aligned} \Gamma_1(x,y,t) =& -\frac{1}{4} + \frac{3}{4}\left(1 + \tanh((x+y+\beta t)/2)\right) - \frac{3}{8}\left(1 + \tanh((x+y+\beta t)/2)\right)^2, \\ \Gamma_2(x,y,t) =& -\frac{1}{4} + \frac{3}{4}\left(1 + \coth((x+y+\beta t)/2)\right)\left[1 - \frac{1}{2}\left(1 + \coth((x+y+\beta t)/2)\right)\right], \\ \Gamma_3(x,y,t) =& \frac{3}{4}\left(1 + \tanh((x+y-\beta t)/2)\right) - \frac{3}{8}\left(1 + \tanh((x+y-\beta t)/2)\right)^2, \\ \Gamma_4(x,y,t) =& \frac{3}{4}\left(1 + \coth((x+y+\beta t)/2)\right)\left[1 - \frac{1}{2}\left(1 + \coth((x+y+\beta t)/2)\right)\right]. \end{aligned} \tag{3.7}$$

Figure 1(a),(b) illustrates the time-dependent behavior of the exact solutions, which can be described by two fundamental components: (a) Γ_1 and (b) Γ_3. The parameter β is set to 1.20, and t varies from 0 to 50 with a step size of 10.

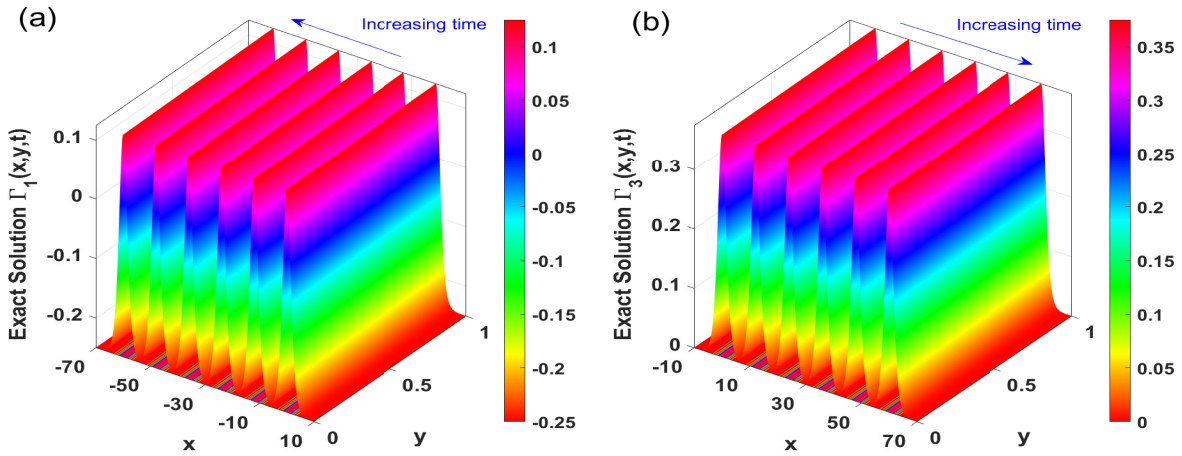

Figure 1. The time evolution of the exact solutions can be described by two components: (a) Γ_1 and (b) Γ_3. The parameter is supplied for the parameter values of $\beta = 1.20$, where t ranges from 0 to 50 with an increment of 10.

(2) When given the values of $\mu_0 = 1$, $\mu_1 = 0$ and $\mu_2 = -1$, two distinct cases arise. The proposed solutions are as follows:

$$\begin{aligned}
\Gamma_5(x,y,t) =& \frac{3}{2} - \frac{3}{2}\tanh^2((x+y-4\beta t)),\\
\Gamma_6(x,y,t) =& \frac{3}{2} - \frac{3}{2}\coth^2((x+y-4\beta t)),\\
\Gamma_7(x,y,t) =& -1 - \frac{3}{2}\left(\tanh^2((x+y+16\beta t)) + \coth^2((x+y+16\beta t))\right),\\
\Gamma_8(x,y,t) =& \frac{1}{2} - \frac{3}{2}\tanh^2(4\beta t + x + y),\\
\Gamma_9(x,y,t) =& \frac{1}{2} - \frac{3}{2}\coth^2(4\beta t + x + y),\\
\Gamma_{10}(x,y,t) =& 3 - \frac{3}{2}\tanh^2(16\beta t - x - y) - \frac{3}{2}\coth^2(16\beta t - x - y).
\end{aligned} \tag{3.8}$$

Observe the precise solutions time history depicted in Figure 2(a),(b) respectively labeled as Γ_5 and Γ_8. The parameter value is $\beta = 1.20$, and time values range from 0 to 10 in step 2. It is imperative to note that the parameter value has already been supplied.

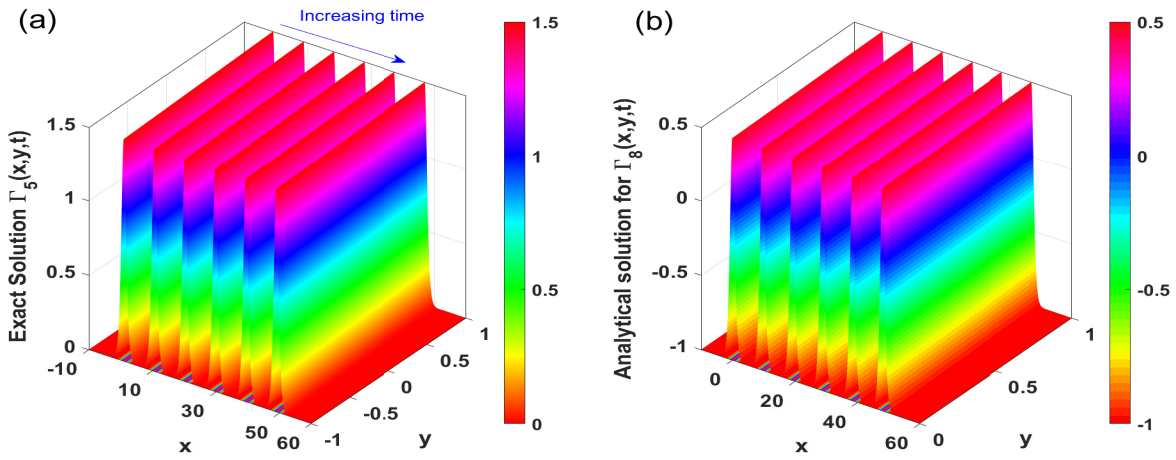

Figure 2. Temporal progression of precise solutions denoted as (a) Γ_5 and (b) Γ_8. The parameter is supplied for the parameter value of $\beta = 1.20$ and the range of values for time is defined as $t = 0 : 2 : 10$.

(3) When $\mu_0 = \frac{1}{2}$, $\mu_1 = 0$, and $\mu_2 = \frac{1}{2}$, the solutions are provided as follows

$$\begin{aligned}
\Gamma_{11}(x,y,t) &= -\frac{3}{8}\left(1 + (\sec(x+y+\beta t) \pm \tan(x+y+\beta t))^2\right),\\
\Gamma_{12}(x,y,t) &= \frac{1}{4} - \frac{3}{8}\Big((\sec(x+y+4\beta t) + \tan(x+y+4\beta t))^2 + \\
&\quad (\sec(x+y+4\beta t) + \tan(x+y+4\beta t))^{-2}\Big).
\end{aligned} \tag{3.9}$$

(4) When $\mu_0 = \frac{1}{2}$, $\mu_1 = 0$, and $\mu_2 = -\frac{1}{2}$, the solutions are provided as follows

$$\begin{aligned}
\Gamma_{13}(x,y,t) &= \frac{1}{8}\left(-3\tanh^2\left(\frac{1}{2}(4\beta t + x + y)\right) - 3\coth^2\left(\frac{1}{2}(4\beta t + x + y)\right) - 2\right),\\
\Gamma_{14}(x,y,t) &= \frac{1}{8} - \frac{3}{8}(\coth(\beta t + x + y) + \operatorname{csch}(\beta t + x + y))^2,\\
\Gamma_{15}(x,y,t) &= \frac{1}{8} - \frac{3}{8}(\coth(\beta t + x + y) + \operatorname{csch}(\beta t + x + y))^{-2},\\
\Gamma_{16}(x,y,t) &= \frac{1}{8}\left(1 - 3\coth^2\left(\frac{1}{2}(\beta t + x + y)\right)\right),\\
\Gamma_{17}(x,y,t) &= \frac{3}{8}\operatorname{sech}^2\left(\frac{1}{2}(\beta t - x - y)\right).
\end{aligned} \tag{3.10}$$

Figure 3(a),(b) undeniably demonstrates the time history of two precise solutions, expertly labeled as (a) Γ_{11} and (b) Γ_{17} respectively. The provided parameter value is $\beta = 1.20$, and the range of values for t is unequivocally defined as $t = 0 : 2 : 10$.

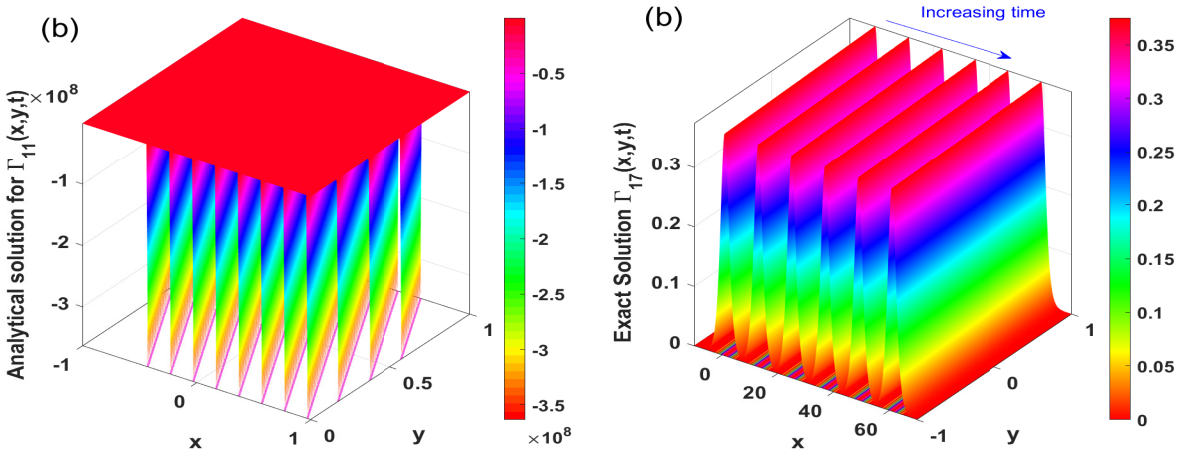

Figure 3. Temporal progression of precise solutions denoted as (*a*) Γ_{11} and (*b*) Γ_{17}. The parameter is supplied for the parameter value of $\beta = 1.20$ and the range of values for t is defined as $t = 0 : 2 : 10$.

The solution to Eq (3.4) can be determined by using the generalized algebraic technique with $M = 2$.

$$\Phi(\zeta) = \rho_0 + \rho_1\psi(\zeta) + \rho_2\psi(\zeta)^2 + \frac{s_1}{\psi(\zeta)} + \frac{s_2}{\psi(\zeta)^2}, \tag{3.11}$$

where $\psi(\zeta)$ represents a solution of the following equation:

$$\psi'(\zeta) = \sqrt{\gamma_0 + \gamma_1\psi(\zeta) + \gamma_2\psi^2(\zeta) + \gamma_3\psi^3(\zeta) + \gamma_4\psi^4(\zeta)}, \tag{3.12}$$

where Table 1 contains a listing of all possible values for γ_j, $j = 0, 1, 2, 3, 4$. In Table 1, one can find a comprehensive list of potential values for γ_j, where j can be 0, 1, 2, 3 or 4. To determine the coefficients $\rho_0, \rho_1, \rho_2, s_1, s_2$ and α for all scenarios mentioned before, we used a mathematical software tool called Mathematica to derive the values. In this section, we will present the analytical solutions to Eq (3.4) by using the generalized algebraic technique and incorporating various alternative values for γ_k, where k ranges from 0 to 4.

(5) If $\gamma_0 = 0, \gamma_1 = 0, \gamma_2 > 0, \gamma_3 = 0$ and $\gamma_4 < 0$, then

$$\begin{aligned} \Gamma_{18}(x, y, t) &= \frac{3}{2}\gamma_2 \ \mathrm{sech}^2\left(\sqrt{\gamma_2}\,(x + y - 4\beta\gamma_2\, t)\right), \\ \Gamma_{19}(x, y, t) &= -\gamma_2 + \frac{3}{2}\gamma_2 \ \mathrm{sech}^2\left(\sqrt{\gamma_2}\,(x + y - 4\beta\gamma_2\, t)\right). \end{aligned} \tag{3.13}$$

(6) If $\gamma_0 = \dfrac{\gamma_2^2}{4\gamma_4 4}$, $\gamma_1 = 0$, $\gamma_2 < 0$, $\gamma_3 = 0$ and $\gamma_4 > 0$, then

$$\begin{aligned}
\Gamma_{20}(x,y,t) =& 3\gamma_2 \operatorname{csch}^2\left(\sqrt{2}\sqrt{-\gamma_2}\,(8\beta\gamma_2 t + x + y)\right),\\
\Gamma_{21}(x,y,t) =& \frac{3}{4}\gamma_2\left[\tanh^2\left(\frac{\sqrt{-\gamma_2}\,(2\beta\gamma_2 t + x + y)}{\sqrt{2}}\right) - 1\right],\\
\Gamma_{22}(x,y,t) =& \frac{1}{4}\gamma_2\left(3\tanh^2\left(\frac{\sqrt{-\gamma_2}(-2\beta\gamma_2 t + x + y)}{\sqrt{2}}\right) - 1\right),\\
\Gamma_{23}(x,y,t) =& \frac{3}{4}\gamma_2 \operatorname{csch}^2\left(\frac{\sqrt{-\gamma_2}\,(2\beta\gamma_2 t + x + y)}{\sqrt{2}}\right),\\
\Gamma_{24}(x,y,t) =& \frac{1}{4}\gamma_2\left(3\tanh^2\left(\frac{\sqrt{-\gamma_2}(-8\beta\gamma_2 t + x + y)}{\sqrt{2}}\right)\right.\\
&\left. + 3\coth^2\left(\frac{\sqrt{-\gamma_2}(-8\beta\gamma_2 t + x + y)}{\sqrt{2}}\right) + 2\right).
\end{aligned} \tag{3.14}$$

(7) If $\gamma_0 = 0$, $\gamma_1 = 0$, $\gamma_2 > 0$, $\gamma_3 \neq 0$, and $\gamma_4 = 0$, then

$$\begin{aligned}
\Gamma_{25}(x,y,t) =& \frac{3}{8}\gamma_2 \operatorname{sech}^2\left(\frac{1}{2}\sqrt{\gamma_2}(-\beta\gamma_2 t + x + y)\right),\\
\Gamma_{26}(x,y,t) =& -\frac{\gamma_2}{4} + \frac{3}{8}\gamma_2 \operatorname{sech}^2\left(\frac{1}{2}\sqrt{\gamma_2}(\beta\gamma_2 t + x + y)\right).
\end{aligned} \tag{3.15}$$

(8) If $\gamma_0 = 0$, $\gamma_1 = 0$, $\gamma_2 < 0$, $\gamma_3 = 0$ and $\gamma_4 > 0$, then

$$\begin{aligned}
\Gamma_{27}(x,y,t) =& \frac{3}{2}\gamma_2 \sec^2\left(\sqrt{-\gamma_2}(-4\beta\gamma_2 t + x + y)\right),\\
\Gamma_{28}(x,y,t) =& \frac{3}{2}\gamma_2 \sec^2\left(\sqrt{-\gamma_2}(4\beta\gamma_2 t + x + y)\right) - \gamma_2.
\end{aligned} \tag{3.16}$$

(9) If $\gamma_0 = \dfrac{\gamma_2^2}{4\gamma_4}$, $\gamma_1 = 0$, $\gamma_2 > 0$, $\gamma_3 = 0$ and $\gamma_4 > 0$, then

$$\begin{aligned}
\Gamma_{29}(x,y,t) =& -\frac{3}{4}\gamma_2 \tan^2\left(\frac{\sqrt{\gamma_2}(8\beta\gamma_2 t + x + y)}{\sqrt{2}}\right)\\
&- \frac{1}{4}3\gamma_2 \cot^2\left(\frac{\sqrt{\gamma_2}(8\beta\gamma_2 t + x + y)}{\sqrt{2}}\right) - \frac{3\gamma_2}{2},\\
\Gamma_{30}(x,y,t) =& -\frac{1}{4}3\gamma_2 \tan^2\left(\frac{\sqrt{\gamma_2}(2\beta\gamma_2 t + x + y)}{\sqrt{2}}\right) - \frac{3\gamma_2}{4},\\
\Gamma_{31}(x,y,t) =& -\frac{1}{4}3\gamma_2 \cot^2\left(\frac{\sqrt{\gamma_2}(2\beta\gamma_2 t + x + y)}{\sqrt{2}}\right) - \frac{3\gamma_2}{4},\\
\Gamma_{32}(x,y,t) =& -\frac{1}{4}3\gamma_2 \tan^2\left(\frac{\sqrt{\gamma_2}(-2\beta\gamma_2 t + x + y)}{\sqrt{2}}\right) - \frac{\gamma_2}{4},\\
\Gamma_{33}(x,y,t) =& -\frac{1}{4}3\gamma_2 \cot^2\left(\frac{\sqrt{\gamma_2}(-2\beta\gamma_2 t + x + y)}{\sqrt{2}}\right) - \frac{\gamma_2}{4}.
\end{aligned} \tag{3.17}$$

In the respective scenarios, the solutions represented by Ψ are equivalent to Γ, whereas β represents arbitrary constants. This discussion will encompass the couple-breaking soliton equation, which incorporates a constant denoted as β. The equations mentioned above delineate the interplay between a prolonged wave propagating down the x axis and a Riemann wave that traverses the y axis. The symbol α is employed to denote the velocity of the singularity. The surface plots in Figure 1 shows the soliton solutions, which are shown as $(a)\,\Gamma_1(x, y, t)$ and $(b)\,\Gamma_3$, for all times between $t = 0$ and 50. Additionally, Figure 2 shows the 3D wave profiles for the soliton solutions Γ_5 and Γ_8 given $\beta = 1.2$ and t ranging from 0 to 10. The surface plots depicted in the solution illustrate the wave profile corresponding to the dazzling type.

4. Numerical solution

In order to obtain precise analytical solutions for the ODE represented by Eq (3.4), we utilize a range of numerical methods. Taking Γ_7 as a case study, we establish the values of Φ and Θ as 0 at the endpoint where $\zeta = 0$. Subsequently, we make initial approximations for the values of Φ_ζ and Θ_ζ. At the initial time $t = 0$, we employ nonlinear shooting and boundary value problem (BVP) methods to determine the second boundary condition $\Phi = 0$ at a designated remaining endpoint within the domain. After acquiring the numerical data, we proceeded to compare it with the analytical solution denoted as Γ_7 at the initial time $t = 0$. The numerical solution can be obtained by utilizing the FSOLVE and ODE15s functions in MATLAB [58]. The discretized form of the resulting ODE given by Eq (3.4), which represents the equation in a discrete manner, i.e.,

$$-\alpha\,\Phi + 2\beta\,\Theta^2 + 2\beta\,\Phi^2 + \frac{\beta}{\delta\zeta^2}\,(\Phi_{i+1} - 2\Phi_i + \Phi_{i-1}) = 0 \tag{4.1}$$

is subjected to the shooting method. In order to verify the accuracy of the analytical solution, the shooting method was applied and the obtained numerical solutions were compared with the analytical solution. Figure 4 illustrates the comparison between the analytical and numerical solutions, which shows that all of the numerical methods used yield consistent results with the analytical solution. Furthermore, the numerical solution obtained can be used as an initial condition for the numerical scheme presented in the following section. At time $t = 25$, we have two solutions to present: The solitary traveling-wave solution and the numerical solution, as depicted in Figure 5(a),(b). These solutions were obtained utilizing the parameter value $\beta = 1.2$, with x ranging from 0 to 20 and y ranging from 0 to 1. The grid size has been set at $N = 3200$ and $J = 100$.

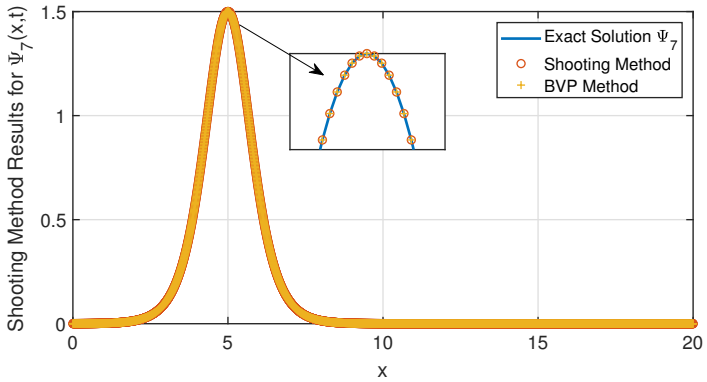

Figure 4. Comparison of the evaluation of Γ_7 at $t = 0$ by using analytical and numerical methods. The parameter is supplied for the parameter value of β set to 1.2; the range of x is from 0 to 20, and the total number of observations is $N = 3200$.

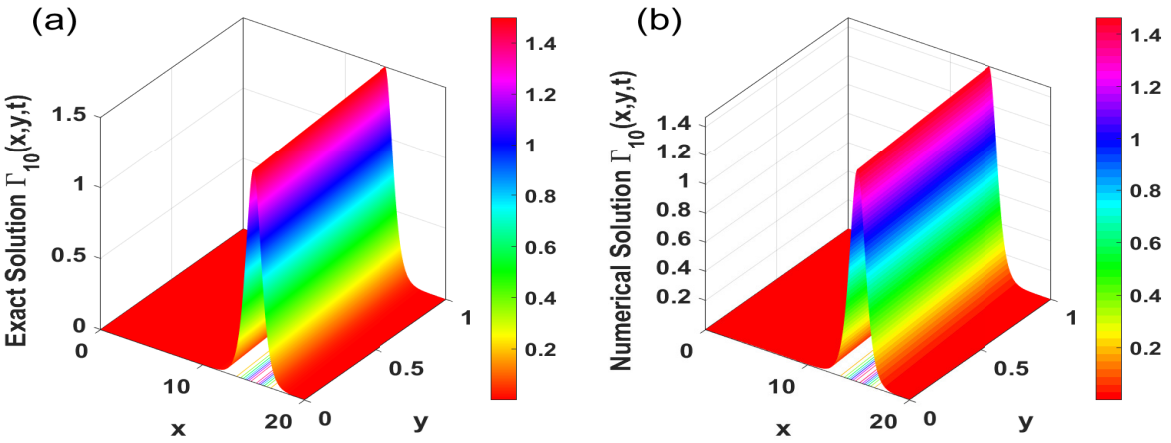

Figure 5. The solitary traveling-wave and numerical solutions at time $t = 25$, as obtained by using the parameter value $\beta = 1.2$, x ranging from 0 to 20, y ranging from 0 to 1 and a grid size of $N = 3200$ with $J = 100$.

In order to compute the numerical solutions of system (1.1) over the rectangular domain $[a, b] \times [0, 1]$, the finite difference approach can be employed. The horizontal extent of the rectangle, as measured along the x direction, is denoted by the variables a and b for the starting and finishing points, respectively. The rectangular region defined by the interval $[a, b]$ on the x axis and the interval $[0, 1]$ on the y direction is partitioned into a grid of $(N + 1) \times (J + 1)$ mesh points. The points are organized in a specific manner:

$$x_i = a + i\,\Delta x, \qquad i = 0, 1, 2, \ldots, N,$$
$$y_j = j\,\Delta y, \qquad j = 0, 1, 2, \ldots, J.$$

The step sizes in the x and y domains are represented by Δx and Δy, respectively. To transform the system described by Eq (1.1) into a system of ODEs, the spatial derivatives are discretized while maintaining the continuity of the time derivative. Successful execution of this procedure leads to

achieving the intended results.

$$\begin{aligned}\Gamma_t|_{i,j}^n =& -\frac{2\beta}{\Delta x}\left[\Gamma_{i+\frac{1}{2},j}^{n+1}(\Psi_{i+1,j}^{n+1}-\Psi_{i-1,j}^{n+1})+\Psi_{i+\frac{1}{2},j}^{n+1}(\Gamma_{i+1,j}^{n+1}-\Gamma_{i-1,j}^{n+1})\right]\\ &-\frac{\beta}{2\Delta y}\delta_x^2(\Gamma_{i,j+1}^{n+1}-\Gamma_{i,j-1}^{n+1}),\\ 0 =& \frac{1}{2\Delta x}(\Psi_{i+1,j}^{n+1}-\Psi_{i-1,j}^{n+1})-\frac{1}{2\Delta y}(\Gamma_{i,j+1}^{n+1}-\Gamma_{i,j-1}^{n+1}),\end{aligned} \tag{4.2}$$

where

$$\delta_x^2\Gamma_{i,j}^{n+1} = \left(\Gamma_{i+1,j}^{n+1}-2\Gamma_{i,j}^{n+1}+\Gamma_{i-1,j}^{n+1}\right).$$

According to the boundary conditions, we have

$$\begin{aligned}&\Gamma_x(a,\,y,\,t)=\Gamma_x(b,\,y,\,t)=0, \qquad \forall y,\\ &\Gamma_y(x,\,0,\,t)=\Gamma_y(x,\,1,\,t)=0, \quad \forall x.\end{aligned} \tag{4.3}$$

The use of boundary constraints allows for the assessment of spatial derivatives at domain boundaries by employing virtual points. Several factors determine the initial conditions:

$$\Gamma_{10}(x,y,t=0) = \frac{3}{2}\gamma_2\ \mathrm{sech}^2\left(\sqrt{\gamma_2}\,(x+y+x0)\right), \tag{4.4}$$

where γ_2 is a positive value selected by the user. The parameter values remain constant for all of the numerical results reported in this section, as follows: $\beta = 0.1$, $x0 = -5.0$, $y = 0 \to 1$, $x = 0 \to 20$ and $t = 0 \to 25$. It is worth mentioning that the DDASPK solver [59] was used to solve the system (4.2). This FORTRAN software is known for its ability to solve ODEs efficiently. To solve the system, a regressive differentiation method was employed, which required an LU-factorization approximation of the Jacobian matrix of the linearized system. This was necessary because there was no initial condition available for the space derivatives. The numerical results obtained are considered satisfactory and the figures presented below will help in understanding them. Figure 6(a),(b) shows three-dimensional representations of both the analytical (on the left) and numerical (on the right) solutions, Γ_{10}. The determination of parameter values involved applying $\beta = 0.1$, $x0 = -5.0$, $y = 0 \to 1$, $x = 0 \to 20$, $t = 0 \to 25$, $J = 100$ and $N = 3200$. Figure 7 represents the changes that occurred within the specified time range of the numerical results. Here, we fixed the value of $y = 0.5$ at $t = 25$; doing so is crucial. After analyzing the wave, the numerical and analytical solutions are pretty similar. The parameters were selected using a methodical approach, which included the following: $\beta = 0.1$, $x0 = -5.0$, $x = 0 \to 20$, $t = 0 \to 25$, $J = 100$ and $N = 3200$.

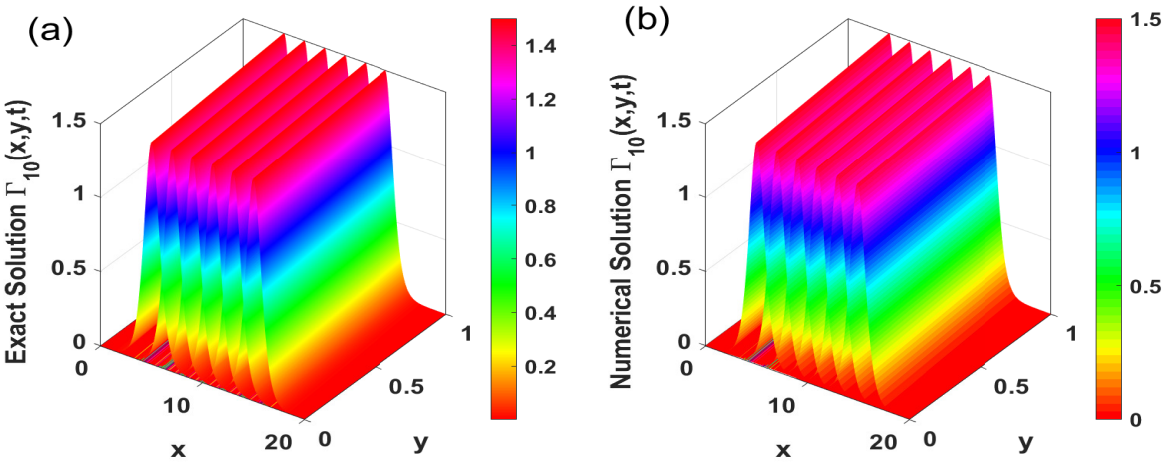

Figure 6. The 3D representations showing both the analytical (left) and numerical (right) solutions, Γ_{10}. The determination of parameter values involved applying $\beta = 0.1$, $x0 = -5.0$, $y = 0 \to 1$, $x = 0 \to 20$, $t = 0 \to 25$, $J = 100$ and $N = 3200$.

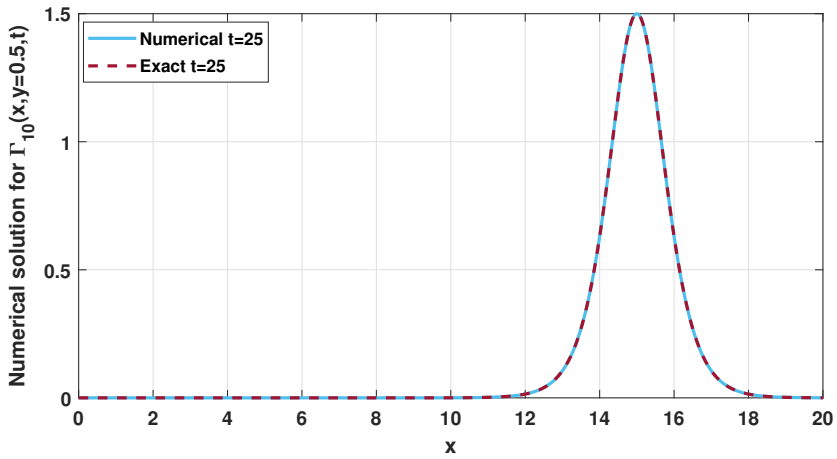

Figure 7. Illustration of changes in the time range of the numerical results. It is crucial to maintain a constant value of $y = 0.5$ at $t = 25$. Upon analyzing the wave, it is clear that there is a significant resemblance between the numerical and analytical solutions. The parameter values were determined by using a systematic process: $\beta = 0.1$, $x0 = -5.0$, $x = 0 \to 20$, $t = 0 \to 25$, $J = 100$ and $N = 3200$.

The Fourier analysis, commonly referred to as the von Neumann analysis, was the only method employed to evaluate the stability of scheme (4.2). It is crucial to acknowledge that this strategy is solely applicable to linear schemes. Therefore, the scheme must be assessed in its linear form to ensure its stability:

$$\begin{aligned} &\Gamma_t + 4\beta\Gamma\Psi_x + 4\beta\Gamma_x\Psi + \beta\Gamma_{xxy} = 0, \\ &\Psi_x - \Gamma_y = 0. \end{aligned} \tag{4.5}$$

By examining the second equation of system (3.3), it can be deduced that Γ is equal to Ψ. Hence, the

initial equation of Eq (4.5) is expressed as

$$\Gamma_t + 8\beta\Gamma\Gamma_x + \beta\Gamma_{xxy} = 0, \tag{4.6}$$

where β represents a fixed value. To effectively implement the Fourier stability approach, it is imperative to convert Eq (4.6) into a linear equation that is fully compatible with the approach being used.

$$\Gamma_t + d_0\Gamma_x + \beta\Gamma_{xxy} = 0, \tag{4.7}$$

where $d_0 = 8\beta\Gamma$ is a constant quantity given by

$$d_0 = \max_{\substack{1\le i\le N\\ 1\le j\le J}} \left(8\beta\Gamma_{i,j}^n\right).$$

Using the finite difference method, Eq (4.7) is given by

$$\begin{aligned}\Gamma_{i,j}^n =&\Gamma_{i,j}^{n+1} + D_0\Gamma_{i+1,j}^{n+1} - D_0\Gamma_{i-1,j}^{n+1} + D_1\left(\Gamma_{i+1,j+1}^{n+1} - 2\Gamma_{i,j+1}^{n+1} + \Gamma_{i-1,j+1}^{n+1}\right)\\ &- D_1\left(\Gamma_{i+1,j-1}^{n+1} - 2\Gamma_{i,j-1}^{n+1} + \Gamma_{i-1,j-1}^{n+1}\right),\end{aligned} \tag{4.8}$$

where $D_0 = \frac{d_0\Delta t}{2\Delta x}$, $D_1 = \frac{\beta\Delta t}{2\Delta y}$.
It is important to note that the conditions at the boundary will not be factored into consideration. Suppose that $x_i = i\Delta x, y_j = j\Delta y$ and $t_n = n\Delta t$; then

$$\begin{gathered}\Gamma_{i,j}^n = \mu^n \exp(\iota\,\xi\pi i\Delta x)\, \exp(\iota\,\eta\pi j\Delta y) \quad \text{and then} \quad \Gamma_{i,j}^{n+1} = \mu\Gamma_{i,j}^n,\\ i = 1, 2, \ldots, N, \quad j = 1, 2, \ldots, M \text{ and } \forall n.\end{gathered} \tag{4.9}$$

By inserting Eq (4.9) into Eq (4.7), we obtain the following outcomes:

$$\Gamma_{i,j}^n = \mu\Gamma_{i,j}^n + 2D_0\sin(\xi\pi\Delta x)\mu\Gamma_{i,j}^n - 8\iota D_1\sin^2\left(\frac{\xi\pi\Delta x}{2}\right)\sin(\eta\pi\Delta y)\,\mu\Gamma_{i,j}^n. \tag{4.10}$$

Hence,

$$1 = \left(1 + 2D_0\sin(\xi\pi\Delta x) - 8\iota D_1\sin^2\left(\frac{\xi\pi\Delta x}{2}\right)\sin(\eta\pi\Delta y)\right)\mu. \tag{4.11}$$

Let

$$\nu = 2D_0\sin(\xi\pi\Delta x) - 8\iota D_1\sin^2\left(\frac{\xi\pi\Delta x}{2}\right)\sin(\eta\pi\Delta y). \tag{4.12}$$

Equation (4.11) can be rewritten as

$$|\mu| = \left|\frac{1}{1+\nu}\right| \le 1. \tag{4.13}$$

Our study unequivocally demonstrates that the scheme under consideration is stable and strictly adheres to the Fourier stability criteria. It is imperative to ensure that the magnitude of μ remains less than one and we can confidently assert that the system satisfies this critical criterion. The equation depicted in Eq (4.11) provides unequivocal evidence that the absolute value of μ is less than one, ensuring that the numerical system remains stable under all possible conditions.

To determine the order of accuracy of the scheme (4.2), the Taylor series is utilized and the truncation error is assessed. It is assumed that:

$$e_{i,j}^{n+1} = \Gamma_{i,j}^{n+1} - \Gamma\left(x_i, y_j, t_{n+1}\right). \tag{4.14}$$

To analyze errors at a specific location and time (x_i, y_j, t_{n+1}), we use the error term $e_{i,j}^{n+1}$. The estimated solution is denoted as $\Gamma_{i,j}^{n}$, while the analytical solution is represented as $\Gamma\left(x_i, y_j, t_{n+1}\right)$ in the context of this study. The final result can be found by substituting Eq (4.14) into scheme (4.8).

$$\begin{aligned} e_{i,j}^{n} =& e_{i,j}^{n+1} + D_0 e_{i+1,j}^{n+1} - D_0 e_{i-1,j}^{n+1} + D_1\left(e_{i+1,j+1}^{n+1} - 2e_{i,j+1}^{n+1} + e_{i-1,j+1}^{n+1}\right) \\ & - D_1\left(e_{i+1,j-1}^{n+1} - 2e_{i,j-1}^{n+1} + e_{i-1,j-1}^{n+1}\right) - \Delta t T_{i,j}^{n}, \end{aligned} \tag{4.15}$$

where D_0 and D_1 are defined as $\frac{d_0\Delta t}{2\Delta x}$ and $\frac{\beta\Delta t}{2\Delta y}$, respectively. The truncation error of $T_{i,j}^{n}$ may be expressed by using the method described by $T_{i,j}^{n}$ as follows:

$$\begin{aligned} T_{i,j}^{n} =& \Gamma\left(x_i, y_j, t_{n+1}\right) + D_0\Gamma\left(x_{i+1}, y_j, t_{n+1}\right) - D_0\Gamma\left(x_{i-1}, y_j, t_{n+1}\right) \\ & + D_1\left(\Gamma\left(x_{i+1}, y_{j+1}, t_{n+1}\right) - 2\Gamma\left(x_i, y_{j+1}, t_{n+1}\right) + \Gamma\left(x_{i-1}, y_{j+1}, t_{n+1}\right)\right) \\ & - D_1\left(\Gamma\left(x_{i+1}, y_{j-1}, t_{n+1}\right) - 2\Gamma\left(x_i, y_{j-1}, t_{n+1}\right) + \Gamma\left(x_{i-1}, y_{j-1}, t_{n+1}\right)\right). \end{aligned} \tag{4.16}$$

Hence,

$$T_{i,j}^{n} \leq \frac{\Delta t}{2}\Gamma_{tt}\left(x_i, y_j, \eta 0_{n+1}\right) - \frac{\Delta x\Delta y}{4}\Gamma_{xxyy}\left(\eta 1_i, \eta 2_j, t_{n+1}\right) - \frac{\Delta x^2}{6}\Gamma_{xxx}\left(\eta 1_i, y_j, t_{n+1}\right), \tag{4.17}$$

where $\eta 0_{n+1} \in (t_n, t_{n+1})$, $\eta 1_i \in (x_{i-1}, x_{i+1})$, and $\eta 2_j \in \left(y_{j-1}, y_{j+1}\right)$. Thus, the numerical scheme's truncation error is $T_{i,j}^{n} = O(\Delta t) + O(\Delta y^2) + O\left(\Delta x^2\right)$. Consequently, every step's truncation error is indicated by

$$T_{i,j}^{n} = O\left(\Delta t, \Delta y^2, \Delta x^2\right).$$

We can perform a series of computations using the initial data and refining them with distinct meshes so that (Δx, Δy, $\Delta t \to 0$). To determine if a numerical scheme is convergent within a chosen domain D, we can evaluate each fixed point $(x^*, y^*, t^*) \in D$ and verify if $(x_i, y_j, t_n) \to (x^*, y^*, t^*)$; then, $\Gamma_{i,j}^{n} = \Gamma(x^*, y^*, t^*)$. Earlier, we showed that the implicit schema guarantees unconditional stability. Now, to prove its unconditional convergence, please continue reading. Suppose that the error is denoted by e. It is provided by

$$e_{i,j}^{n} = \Gamma_{i,j}^{n} - \Gamma\left(x_i, y_j, t_n\right). \tag{4.18}$$

Now, $\Gamma_{i,j}^{n}$ completely satisfies the conditions of the scheme (Eq (4.8)), whereas $\Gamma\left(x_i, y_j, t_n\right)$ ignores the error revealed by the truncation error. Hence,

$$\begin{aligned} e_{i,j}^{n} =& e_{i,j}^{n+1} + D_0 e_{i+1,j}^{n+1} - D_0 e_{i-1,j}^{n+1} + D_1\left(e_{i+1,j+1}^{n+1} - 2e_{i,j+1}^{n+1} + e_{i-1,j+1}^{n+1}\right) \\ & - D_1\left(e_{i+1,j-1}^{n+1} - 2e_{i,j-1}^{n+1} + e_{i-1,j-1}^{n+1}\right) - \Delta t T_{i,j}^{n}, \end{aligned} \tag{4.19}$$

where $D_0 = \frac{d_0\Delta t}{2\Delta x}$, $D_1 = \frac{\beta\Delta t}{2\Delta y}$. Assume that the maximum error for the time step is defined as follows:

$$E^{n} = \max\left\{\left|e_{i,j}^{n}\right|, \forall i, j \text{ and } n \geq 0\right\}. \tag{4.20}$$

Thus, the result of applying Eq (4.20) in Eq (4.19) is

$$e_{i,j}^{n+1} \leq E^n + \Delta t T_{i,j}^n; \tag{4.21}$$

then, for each $i = 1, \ldots, N$, $j = 1, \ldots, M$, we obtain

$$E^{n+1} \leq E^n + \Delta t T_{i,j}^n. \tag{4.22}$$

We can start by using the given initial condition to determine that $E^0 = 0$. With this, we can rewrite the inequality as follows:

$$E^1 \leq E^0 + \Delta t T_{i,j}^n = \Delta t T_{i,j}^n \quad \Rightarrow \quad E^2 \leq E^1 + \Delta t T_{i,j}^n \leq 2\Delta t T_{i,j}^n,$$

and so on; we have

$$E^{n+1} \leq n \times \Delta t T_{i,j}^n. \tag{4.23}$$

5. Result and discussion

This study focused on the use of effective methodologies and the resulting impressive results in solving Eq (1.1). To obtain precise solutions, two methods were utilized, namely, the generalized indirect algebraic and modified S-expansion methods. Figures 1–3 illustrate the solitary wave solutions for the parameters $\beta = 1.2$, $N = 100$ and $M = 3200$. The accuracy of the analytical solutions was then confirmed by performing numerical validation using the converted system (4.2). The primary findings, which provide a direct comparison between the analytical and numerical solutions, are presented in Figure 8 and Table 3. These results are significant, as they demonstrate the effectiveness of the employed methodologies and provide further insights for future studies. Through the investigation mentioned earlier, it is clear that the solutions share a significant level of resemblance, with errors decreasing considerably as the values of Δx and Δy approach zero. To maintain stability, it is crucial to keep the parameter β constant across all numerical schemes. Any alterations to this value have the potential to cause instability and should be avoided.

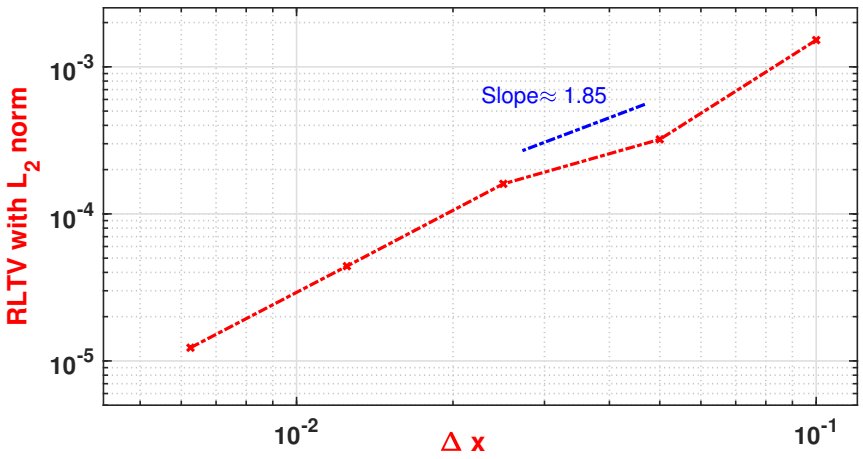

Figure 8. Convergence records based on Δx, as obtained by utilizing the l_2 norm relative error from Table 3. As for the variable y, we specifically selected the value of 0.5 at $t = 25$ and $x = 0 \rightarrow 20$.

Table 3. The relative error formula results applied to measure the error with a fixed $\Delta t = 1 \times 10^{-2}$ at a specific time $t = 25$.

Δx	RLTV	CPU
1.0×10^{-1}	1.5×10^{-3}	56.0 s
5.0×10^{-2}	3.2×10^{-4}	133.36 s
2.5×10^{-2}	1.6×10^{-4}	316.20 s
1.25×10^{-2}	4.4×10^{-5}	619.80 s
6.3×10^{-3}	1.2×10^{-5}	1492.86 s

Figure 1 provides clear representations of the temporal progression of the analytical solutions of (a) Γ_1 over the interval $x = -70 \rightarrow 10$ and (b) Γ_3 over the interval $x = -10 \rightarrow 70$. The graphs were plotted over a time interval of 0 to 50, with a value of β set to 1.2. The time evolution of the analytic solutions is illustrated in Figure 2 for intervals of Γ_5 and Γ_8 from $x = -10$ to $x = 60$. The figure covers a time interval of $t = 0$ to $t = 10$ with $\beta = 1.2$. Similarly, Figure 3 shows the analytical solutions' temporal progression for the intervals of integration for Γ_{11} from $x = -1 \rightarrow 1$ and Γ_{17} from $x = -10 \rightarrow 60$. The time interval of these graphs is also $t = 0$ to $t = 10$, with $\beta = 1.2$. To obtain the numerical results of Eq (4.2), the numerical scheme uses the analytic solution as the starting point. The exact answer for a single traveling wave is shown in Figure 2, along with the solutions obtained by using the shooting approach. These reciprocal solutions operate in unison, indicating that the procedures are genuine and effective. The Taylor series expansion assesses the accuracy of the system, starting with the second order. The numerical approach has second-order accuracy, as demonstrated in Figure 1. The von Neumann analysis provides evidence for the unconditional stability of the numerical system.

Figure 6 illustrates how the precise computational results change over time for a given set of parameters. The parameters used in this scenario are as follows: $\beta = 0.1$, $x0 = -5.0$, y ranging from 0 to 1, x ranging from 0 to 20, t ranging from 0 to 25, $J = 100$ and $N = 3200$. It is clear from the alignment between the analytical and numerical solutions that they are similar. The exact solitary traveling-wave and numerical solutions at time $t = 25$ are illustrated in a three-dimensional representation in Figure 5. The graphical representations effectively demonstrate that the exact solutions exhibit behaviors similar to those observed for the numerical solutions. Figure 7 illustrates the alterations in the time span of the numerical findings. Ensuring a consistent value of $y = 0.5$ at $t = 25$ is of utmost importance. After careful analysis of the wave, it is evident that there is a substantial similarity between the numerical and analytical solutions. The parameter values were established by a systematic procedure: $\beta = 0.1$, $x0 = -5.0$, x ranging from 0 to 20 and t ranging from 0 to 25. The value of J is 100 and the value of N is 3200. The applied strategies' effectiveness is further demonstrated in Table 3 and Figure 8. Table 3 shows the L_2 error and the computational time required to reach time step 25 by using the numerical technique. The augmentation of data points leads to a significant decrease in imprecision while simultaneously increasing the computational resources necessary for their processing. The finite difference technique is a computationally advantageous approach for solving nonlinear partial differential equations because it captures high-error regions effectively by employing an adequate number of data points, thus rapidly reducing the overall error.

6. Conclusions

As part of our investigation, we utilized two techniques, i.e., the generalized indirect algebraic and modified S-expansion techniques, to identify different solitary wave solutions for the couple-breaking soliton equations. We used hyperbolic and trigonometric functions, along with the shooting approach, to obtain these solutions. After constructing a solution, we employed a numerical scheme to solve the problem, completed without any issues. To ensure the accuracy of our results, we conducted a comprehensive analysis of the differences and similarities between the analytical and numerical outcomes. We found that the results were practically identical in how they were obtained, but the finite differences-based approach was more accurate. We also observed a correlation between the total number of points and the relative error, which suggested that the numerical scheme is stable. In summary, the methodologies we applied were effective in performing the computations.

Use of AI tools declaration

The author declares that he has not used artificial intelligence tools in the creation of this article.

Acknowledgments

The author extends their appreciation to the Deanship for Research and Innovation Ministry of Education in Saudi Arabia for funding this research through project number 445-9-637.

Conflict of interest

The author declares that he has no potential conflict of interest that may influence the publication of this article.

References

1. A. Akbulut, S. Islam, H. Rezazadeh, F. Tascan, Obtaining exact solutions of nonlinear partial differential equations via two different methods, *Int. J. Mod. Phys. B*, **36** (2022), 2250041. https://doi.org/10.1142/S0217979222500412
2. W. X. Ma, X. Yong, H. Zhang, Diversity of interaction solutions to the (2+1)-dimensional Ito equation, *Comput. Math. Appl.*, **75** (2018), 289–295. https://doi.org/10.1016/j.camwa.2017.09.013
3. Y. Ozkam, E. Yasar, M. Osman, Novel multiple soliton and front wave solutions for the 3D-Vakhnenko-Parkes equation, *Mod. Phys. Lett. B*, **36** (2022). https://doi.org/10.1142/S0217984922500038
4. M. Bashar, S. Islam, Exact solutions to the (2 + 1)-dimensional Heisenberg ferromagnetic spin chain equation by using modified simple equation and improve F-expansion methods, *Phys. Open*, **5** (2020), 100027. https://doi.org/10.1016/j.physo.2020.100027
5. A. Alharbi, M. Almatrafi, Analytical and numerical solutions for the variant Boussinseq equations, *J. Taibah Univ. Sci.*, **14** (2020), 454–462. https://doi.org/10.1080/16583655.2020.1746575

6. A. Alharbi, M. Almatrafi, Numerical investigation of the dispersive long wave equation using an adaptive moving mesh method and its stability, *Results Phys.*, **16** (2020), 102870. https://doi.org/10.1016/j.rinp.2019.102870
7. A. Alharbi, M. Almatrafi, Riccati-Bernoulli Sub-ODE approach on the partial differential equations and applications, *Int. J. Math. Comput. Sc.*, **15** (2020), 367–388.
8. A. Alharbi, M. Almatrafi, New exact and numerical solutions with their stability for Ito integro-differential equation via Riccati-Bernoulli sub-ODE method, *J. Taibah Univ. Sci.*, **14** (2020), 1447–1456.
9. A. Alharbi, M. Almatrafi, Exact and numerical solitary wave structures to the variant Boussinesq system, *Symmetry*, **12** (2020), 1473.
10. M. Almatrafi, A. Alharbi, C. Tunç, Constructions of the soliton solutions to the good Boussinesq equation, *Adv. Differential Equ.*, **629** (2020). https://doi.org/10.1186/s13662-020-03089-8
11. A. Alharbi, M. Almatrafi, A. Seadawy, Construction of the numerical and analytical wave solutions of the Joseph-Egri dynamical equation for the long waves in nonlinear dispersive systems, *Int. J. Mod. Phys. B*, 2020, 2050289. https://doi.org/10.1142/S0217979220502896
12. A. Alharbi, M. Almatrafi, K. Lotfy, Constructions of solitary travelling wave solutions for Ito integro-differential equation arising in plasma physics, *Results Phys.*, **19** (2020), 103533. https://doi.org/10.1016/j.rinp.2020.103533
13. A. Alharbi, M. Almatrafi, Exact solitary wave and numerical solutions for geophysical KdV equation, *J. King Saud Univ. Sci.*, **6** (2022), 102087. https://doi.org/10.1016/j.jksus.2022.102087
14. S. Zaki, Solitary wave interactions for the modified equal width equation, *Comput. Phys. Commun.*, **126** (2000), 219–231. https://doi.org/10.1016/S0010-4655(99)00471-3
15. A. Wazwaz, The tanh method and the sine-cosine method for solving the KP-MEW equation, *Int. J. Comput. Math.*, **82** (2005), 235–246. https://doi.org/10.1080/00207160412331296706
16. M. Almatrafi, A. Alharbi, A. Seadawy, Structure of analytical and numerical wave solutions for the Ito integro-differential equation arising in shallow water waves, *J. King Saud Univ. Sci.*, **33** (2021), 101375. https://doi.org/10.1016/j.jksus.2021.101375
17. A. Alharbi, M. Faisal, F. Shah, M. Waseem, R. Ullah, S. Sherbaz, Higher order numerical approaches for nonlinear equations by decomposition technique, *IEEE Access*, **7** (2019), 44329–44337. https://doi.org/10.1109/ACCESS.2019.2906470
18. R. Radha, M. Lakshmanan, Dromion like structures in the (2+1)-dimensional breaking soliton equation, *Phys. Lett. A*, **197** (1995). https://doi.org/10.1016/0375-9601(94)00926-G
19. Z. Yan, H. Zhang, Constructing families of soliton-like solutions to a (2+1)-dimensional breaking soliton equation using symbolic computation, *Int. J. Comput. Math. Appl.*, **44** (2002), 1439–1444. https://doi.org/10.1016/S0898-1221(02)00268-7
20. Y. Chen, L. Biao, H. Zhang, Symbolic computation and construction of soliton-like solutions to the (2+1)-dimensional breaking soliton equation, *Commun. Theor. Phys.*, **40** (2003), 137–142. https://dx.doi.org/10.1088/0253-6102/40/2/137
21. Z. Wang, S. Tian, J. Cheng, The $\bar{\partial}$-dressing method and soliton solutions for the three-component coupled Hirota equations, *J. Math. Phys.*, **62** (2021), 093510. https://doi.org/10.1063/5.0046806

22. S. Tian, M. Xu, T. Zhang, A symmetry-preserving difference scheme and analytical solutions of a generalized higher-order beam equation, *Proc. Roy. Soc. Lond. A*, **477** (2021), 20210455. https://doi.org/10.1098/rspa.2021.0455

23. L. Yuan, S. Tian, J. Cheng, Riemann-Hilbert problem and interactions of solitons in the component nonlinear Schrödinger equations, *Stud. Appl. Math.*, **148** (2022), 577–605. https://doi.org/10.1111/sapm.12450

24. S. Dong, Schrödinger equation with the potential $V(r) = Ar^{-4} + Br^{-3} + Cr^{-2} + Dr^{-1}$, *Phys. Scripta*, **64** (2001), 273. https://dx.doi.org/10.1238/Physica.Regular.064a00273

25. S. Dong, The ansatz method for analyzing Schrödinger's equation with three anharmonic potentials in D dimensions, *J. Genet. Couns.*, **15** (2002), 385–395. https://doi.org/10.1023/A:1021220712636

26. Y. Guo, W. Li, S. Dong, Gaussian solitary solution for a class of logarithmic nonlinear Schrödinger equation in (1 + n) dimensions, *Results Phys.*, **44** (2023), 109187. https://doi.org/10.1016/j.rinp.2022.106187

27. R. López, G. Sun, O. C. Nieto, C. Y. Márquez, S. Dong, Analytical traveling-wave solutions to a generalized Gross-Pitaevskii equation with some new time and space varying nonlinearity coefficients and external fields, *Phys. Lett. A*, **381** (2017), 2978–2985. https://doi.org/10.1016/j.physleta.2017.07.012

28. A. Başhan, A mixed algorithm for numerical computation of soliton solutions of the coupled KdV equation: Finite difference method and differential quadrature method, *Appl. Math. Comput.*, **360** (2019), 42–57. https://doi.org/10.1016/j.amc.2019.04.073

29. A. Başhan, A mixed methods approach to Schrödinger equation: Finite difference method and quartic B-spline based differential quadrature method, *Int. J. Optim. Control*, **9** (2019), 223–235. https://doi.org/10.11121/ijocta.01.2019.00709

30. A. Başhan, Y. Uçar, N. M. Yağmurlu, A. Esen, A new perspective for quintic B-spline based Crank-Nicolson-differential quadrature method algorithm for numerical solutions of the nonlinear Schrödinger equation, *Eur. Phys. J. Plus*, **133** (2018), 12. https://doi.org/10.1140/epjp/i2018-11843-1

31. A. Başhan, A novel approach via mixed Crank-Nicolson scheme and differential quadrature method for numerical solutions of solitons of mKdV equation, *Pramana*, **92** (2019), 84. https://doi.org/10.1007/s12043-019-1751-1

32. A. Başhan, A novel outlook to the mKdV equation using the advantages of a mixed method, *Appl. Anal.*, **102** (2023), 65–87. https://doi.org/10.1080/00036811.2021.1947493

33. Y. Peng, E. Krishnan, Two classes of new exact solutions to (2+1)-dimensional breaking soliton equation, *Commun. Theor. Phys.*, **44** (2005), 807–809. https://dx.doi.org/10.1088/6102/44/5/807

34. I. Inan, Generalized Jacobi elliptic function method for traveling wave solutions of (2+1)-dimensional breaking soliton equation, *Cankaya Univ. J. Sci. Eng.*, **7** (2010), 39–50.

35. W. Cheng, Y. Chen, Nonlocal symmetry and exact solutions of the (2+1)-dimensional breaking soliton equation, *Commun. Nonlinear Sci.*, **29** (2015), 198–207. https://dx.doi.org/10.1016/j.cnsns.2015.05.007

36. M. S. Osman, On multi-soliton solutions for the (2+1)-dimensional breaking soliton equation with variable coefficients in a graded-index waveguide, *Comput. Math. Appl.*, **75** (2018), 1–6. https://dx.doi.org/10.1016/j.camwa.2017.08.033

37. J. Manafian, M. Behnam, M. Abapour, Lump-type solutions and interaction phenomenon to the (2+1)-dimensional breaking soliton equation, *Appl. Math. Comput.*, **356** (2019), 13–41. https://dx.doi.org/10.1016/j.amc.2019.03.016

38. M. Kumar, D. Tanwar, Lie symmetries and invariant solutions of (2 + 1)-dimensional breaking soliton equation, *Pranama J. Phys.*, **94** (2020), 23. https://dx.doi.org/10.1007/s12043-019-1885-1

39. H. Baskonus, A. Kumar, G. Wei, Deeper investigations of the (4 + 1)-dimensional Fokas and (2 + 1)-dimensional breaking soliton equations, *Int. J. Mod. Phys. B*, **34** (2020), 2050152. https://dx.doi.org/10.1142/S0217979220501520

40. A. Alharbi, Numerical solutions to two-dimensional fourth order parabolic thin film equations using the Parabolic Monge-Ampere method, *AIMS Math.*, **8** (2023), 16463–16478. https://dx.doi.org/10.3934/math.2023841

41. B. Ren, P. Chu, Dynamics of D'Alembert wave and soliton molecule for a (2+1)-dimensional generalized breaking soliton equation, *Chinese J. Physiol.*, **74** (2021), 296–301. https://dx.doi.org/10.1016/j.cjph.2021.07.025

42. M. Kaplan, A. Akbulut, The analysis of the soliton-type solutions of conformable equations by using generalized Kudryashov method, *Opt. Quant. Electron.*, **53** (2021), 498. https://doi.org/10.1007/s11082-021-03144-y

43. Y. Qin, Y. Gao, Y. Shen, Y. Sun, G. Meng, X. Yu, Solitonic interaction of a variable coefficient (2 + 1)-dimensional generalized breaking soliton equation, *Phys. Scripta*, **88** (2013), 045004. https://dx.doi.org/10.1088/0031-8949/88/04/045004

44. D. Kumar, Application of the modified Kudryashov method to the generalized Schrödinger-Boussinesq equations, *Opt. Quant. Electron.*, **50** (2018), 329. https://doi.org/10.1007/s11082-018-1595-9

45. M. Mirzazadeh, K. Hosseini, K. Dehingia, S. Salahshour, A second-order nonlinear Schrödinger equation with weakly nonlocal and parabolic laws and its optical solitons, *Optic*, **242** (2021), 166911. https://doi.org/10.1016/j.ijleo.2021.166911

46. T. Xia, S. Xiong, Exact solutions of (2 + 1)-dimensional Bogoyavlenskii's Breaking soliton equation with symbolic computation, *Comput. Math. Appl.*, **60** (2010), 919–923. https://doi.org/10.1016/j.camwa.2010.05.037

47. A. Alharbi, M. Almatrafi, M. Abdelrahman, Analytical and numerical investigation for Kadomtsev-Petviashvili equation arising in plasma physics, *Phys. Scripta*, **95** (2020), 045215. https://dx.doi.org/10.1088/1402-4896/ab6ce4

48. A. Alharbi, A Study of traveling wave structures and numerical investigation of two-dimensional Riemann problems with their stability and accuracy, *Comp. Model. Eng. Sci.*, **134** (2023), 2193–2209. https://doi.org/10.32604/cmes.2022.018445

49. W. Ma, Riemann-Hilbert problems and inverse scattering of nonlocal real reverse-spacetime matrix AKNS hierarchies, *Physica D*, **177** (2022), 104522. https://doi.org/10.1016/j.geomphys.2022.104522
50. W. Ma, Nonlocal integrable mKdV equations by two nonlocal reductions and their soliton solutions, *J. Geom. Phys.*, **430** (2022), 133078. https://doi.org/10.1016/j.physd.2021.133078
51. O. Bogoyavlenskiĭ, Overturning solitons in new two-dimensional integrable equations, *Izv. Akad. Nauk SSSR Ser. Mat.*, **53** (1989), 243–257. https://doi.org/10.1070/IM1990v034n02ABEH000628
52. F. Calogero, A. Degasperis, Nonlinear evolution equations solvable by the inverse spectral transform. Pt. I, *Nuovo Cim. B*, **32** (1976), 201–242, https://doi.org/10.1007/BF02727634
53. F. Calogero, A. Degasperis, Nonlinear evolution equations solvable by the inverse spectral transform. II, *Nuovo Cim. B*, **39** (1977), 1–54. https://doi.org/10.1007/BF02738174
54. A. Kazeykina, C. Klein, Numerical study of blow-up and stability of line solitons for the Novikov-Veselov equation, *Nonlinearity*, **30** (2017), 2566. https://dx.doi.org/10.1088/1361-6544/aa6f29
55. B. Sagar, S. Saha, Numerical soliton solutions of fractional (2+1)-dimensional Nizhnik-Novikov-Veselov equations in nonlinear optics, *Int. J. Mod. Phys. B*, **35** (2021), 2150090. http://dx.doi.org/10.1142/S0217979221500909
56. C. Bai, C. Bai, H. Zhao, A new generalized algebraic method and its application in nonlinear evolution equations with variable coefficients, *Z. Naturforsch. A*, **60** (2005), 211–220. https://doi.org/10.1515/zna-2005-0401
57. A. Aasaraai, The application of modified F-expansion method solving the Maccari's system, *J. Adv. Math. Comput. Sci.*, **11** (2015), 1–14. http://dx.doi.org/10.9734/BJMCS/2015/19938
58. L. Shampine, M. Reichelt, The matlab ode suite, *SIAM J. Sci. Comput.*, **18** (1997), 1–22. https://doi.org/10.1137/S1064827594276424
59. P. Brown, A. Hindmarsh, L. R. Petzold, Using Krylov methods in the solution of large-scale differential-algebraic systems, *SIAM J. Sci. Comput.*, **15** (1994), 1467–1488. https://doi.org/10.1137/0915088